Universal Scale-Free Decay of Tracer-Bath Correlations in d-Dimensional Interacting Particle Systems

Davide Venturelli,[1] Pierre Illien,[2] Aurélien Grabsch,[1] and Olivier Bénichou[1]
[1]Sorbonne Université, CNRS, Laboratoire de Physique Théorique de la Matière Condensée (LPTMC), 4 Place Jussieu, 75005 Paris, France
[2]Sorbonne Université, CNRS, Laboratoire PHENIX (Physico-Chimie des Electrolytes et Nanosystèmes Interfaciaux), 4 Place Jussieu, 75005 Paris, France

(Received 19 November 2024; revised 23 June 2025; accepted 27 August 2025; published 15 September 2025)

Quantifying the correlations between the position of a tagged tracer and the density of surrounding bath particles is crucial for understanding tracer diffusion in interacting particle systems, and for characterizing the response properties of the bath. We address this problem analytically for both hard-core and soft-core interactions, using minimal yet paradigmatic models in d spatial dimensions. In both cases, we derive analytical expressions for the spatial correlation profiles in the reference frame of the tracer. We reveal unexpected universal features in their large-distance behavior, characterized by power-law tails with exponents that depend solely on the spatial dimensionality of the system. Beyond these simple models, we demonstrate the robustness of our results across different regimes using particle-based numerical simulations.

DOI: 10.1103/55qy-sflc

Introduction—Assessing the statistics of the displacement of a tagged tracer particle evolving in a complex medium subject to thermal fluctuations is a paradigmatic problem in statistical physics, which found in the last decades numerous applications to microrheology [1–6] and biophysics [7,8] experiments. A basic but powerful approach toward describing tracer diffusion in complex media is to neglect the effect that the tracer exerts on the surrounding bath, which is assumed to remain in equilibrium at all times, and can thus generically be treated as a source of noise [9]. This is exemplified by the celebrated Langevin description of Brownian motion [10], which assumes a large mass disparity between tracer and bath particles [11,12]. However, such effective description naturally breaks down if the tracer particle (TP) and the bath particles have comparable sizes, because then correlations between the tracer position and the density of the surrounding bath assume a relevant role, and can no longer be neglected. Characterizing these correlations is in general a complex many-body problem. However, their knowledge gives full access not only to the TP fluctuations, but also to the response properties of the medium itself, which makes the pursuit of these correlations (at least in approximate forms) valuable.

An ideal and fertile arena for seeking analytical predictions for these correlations is provided by lattice gases, which are arguably among the most emblematic models to study transport properties in interacting particle systems [13,14]. They consist of particles that can jump from one site of the lattice to another, with the constraint that each site can host at most one particle—this minimally models hard-core or excluded-volume interactions. The one-dimensional case, corresponding to the single-file geometry, exemplifies spectacularly how the correlations with the surrounding bath particles induce subdiffusive behavior of the TP displacement [15]. These correlations have recently been computed exactly for the symmetric exclusion process [16] and related (integrable) one-dimensional models [17–19]. In higher dimensions, approximate semi-analytical solutions for these correlations have been key to obtaining the variance of the TP position, particularly in nonequilibrium settings [20–23].

On the other hand, in continuum space, particles are often assumed to evolve according to a system of coupled Langevin equations, featuring two-body interaction potentials that provide a more realistic modeling of their interactions (beyond excluded volume). In the overdamped case, the exact evolution equation of the coarse-grained particle density was derived in seminal works by Dean and Kawasaki [24,25], yet the presence of nonlinear multiplicative noise has so far hindered all efforts toward its exact solution. Conversely, the correction to the diffusion coefficient of a driven TP induced by the bath, as well as the average density profile in the frame of the TP, have only more recently been addressed in [26] by linearizing the coarse-grained equations around a fixed background density. However, this approach typically fails when attempting to interpolate between the Dean-Kawasaki theory and the hard-core particle limit by simply increasing the strength of the two-body potentials [27], which prevents the description of proper hardcorelike repulsive interactions. Besides, computing the correlations between the TP position and

the coarse-grained bath density beyond the average density profile has never been attempted (to the best of our knowledge) within this setting.

Because of the key role played by these correlations in determining the TP statistics, their use in d-dimensional lattice models has been so far mainly instrumental in the description of the TP variance. In this Letter, we focus instead on the stationary TP-bath correlations in their own right, with the aim of analyzing their spatial properties. Indeed, these profiles quantify the variation of the bath density distribution due to a fluctuation of the TP position, thus allowing one to probe the bath's response even far from the TP.

Tracer-bath correlations—We start by defining the TP-bath correlation functions, which are the focus of this Letter, and highlight their importance and intrinsic dynamical nature. Although we will consider them in both discrete and continuous settings, we introduce them here in the continuous case for clarity. We denote by $\{\mathbf{X}_i(t)\}$ the positions of the particles at time t. We single out particle $i = 0$, referred to hereafter as the TP, and denote its displacement by $\mathbf{X}(t) \equiv \mathbf{X}_0(t) - \mathbf{X}_0(0) \equiv \mathbf{X}_0(t)$, adopting the convention $\mathbf{X}_0(0) = 0$. Let $\rho(\mathbf{x}, t)$ denote the density of the other particles ($i \neq 0$), referred to as the bath particles.

We first note that $\mathbf{X}(t)$ and $\rho(\mathbf{x}, t)$ are coupled. Qualitatively, any large displacement $\mathbf{X}(t)$ of the TP in a given direction requires the reorganization of a large number of bath particles, encoded in the density $\rho(\mathbf{X}(t) + \mathbf{r}, t)$ around the tracer. In turn, the dynamics of this reorganization governs that of the TP. The two random variables, $\mathbf{X}(t)$ and $\rho(\mathbf{X}(t) + \mathbf{r}, t)$, are thus coupled, and characterizing this coupling is essential to understanding the transport properties of the tracer and quantifying the perturbation induced by its displacement.

Quantitatively, this coupling is naturally described by the covariance $\mathrm{Cov}\{\mathbf{X}(t), \rho(\mathbf{X}(t) + \mathbf{r}, t)\} \equiv \langle \mathbf{X}(t)\rho(\mathbf{X}(t) + \mathbf{r}, t)\rangle - \langle \mathbf{X}(t)\rangle\langle \rho(\mathbf{X}(t) + \mathbf{r}, t)\rangle = \langle \mathbf{X}(t)\rho(\mathbf{X}(t) + \mathbf{r}, t)\rangle$, since $\langle \mathbf{X}(t)\rangle = 0$. We emphasize that these correlation functions are intrinsically dynamical because they involve the *displacement* $\mathbf{X}(t)$ of the TP rather than its absolute position. Unlike equilibrium quantities, these correlation functions cannot, in practice, be computed from the equilibrium Gibbs measure [28].

Several important questions arise. (i) What is the sign of this coupling? Without loss of generality, consider the projection onto the direction $\hat{\mathbf{e}}_1$, namely $\langle \mathbf{X}(t)\rho(\mathbf{X}(t) + \mathbf{r}, t)\rangle \cdot \hat{\mathbf{e}}_1 = \langle X_t \rho(\mathbf{X}(t) + \mathbf{r}, t)\rangle$, where $X_t = \mathbf{X}(t) \cdot \hat{\mathbf{e}}_1$. A positive sign indicates that an increase in X_t is correlated with an increase in the density at a relative position $\mathbf{r}$ from the tracer, while a negative sign indicates anticorrelation. (ii) What is the range of this coupling? In particular, can short-range interactions lead to long-range reorganization of the bath particles, or do they affect only a finite region of space around the TP? (iii) What is the dynamics of this coupling? Specifically, is this reorganization efficient enough to result in a stationary correlation profile? (iv) What are the relevant parameters controlling this coupling? Does it depend on the nature of the interaction, or on the efficiency of homogenization by diffusion (related to the spatial dimension)?

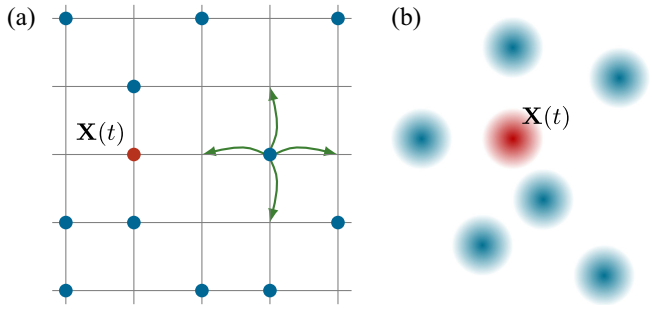

FIG. 1. Schematic representation of the two models considered in this Letter, namely (a) a hard-core d-dimensional lattice gas, where each particle can jump to one of its neighboring sites with equal rates, only if the target site is empty; and (b) a d-dimensional system of Brownian particles interacting via soft pairwise potentials (see the main text). In both cases, we single out the position $\mathbf{X}(t)$ of a tagged tracer particle (red).

In our Letter we provide explicit answers to these key questions by determining and analyzing the TP-bath correlation profiles. To this end, we first derive analytic expressions for these quantities both for a lattice gas model with *hard-core* interactions, and for a system of *soft* interacting Brownian particles. We then find that a power-law behavior at large distances, with a simple algebraic decay exponent depending solely on the spatial dimensionality, encompasses all the interacting particle systems mentioned above—in spite of the intrinsically distinct nature of their interactions, which otherwise prevents their description on an equal footing. Using numerical simulations, we argue that this behavior remains robust beyond the assumptions underlying our analytic derivation, and for Brownian suspensions with strongly repulsive Lennard-Jones-type potentials.

Hard-core lattice gas—We first consider particles evolving on an infinite d-dimensional cubic lattice, with spacing σ. Initially, each site is occupied with probability $\bar{\rho}$. Particles then perform symmetric random walks with nearest-neighbor jumping rate $1/(2d\tau)$ [so that their bare diffusion coefficient is $\sigma^2/(2\tau)$], with the constraint that the target site must be empty [see Fig. 1(a)]. The state of the system at a given time t is specified by the tracer position $\mathbf{X}(t)$, and by the set of occupations $\rho_{\mathbf{r}}(t) = \{0, 1\}$ for each site $\mathbf{r}$. The joint probability distribution $P(\mathbf{X}, \rho_{\mathbf{r}}, t)$ satisfies a master equation $\partial_t P = \mathcal{L}P$, where the well-known form of $\mathcal{L}$ is reported in [29]. Multiplying its two sides by $e^{\boldsymbol{\lambda}\cdot\mathbf{X}}$ and averaging with respect to both $\rho_{\mathbf{r}}$ and $\mathbf{X}$ then yields an evolution equation for the moment generating function $\Psi(\boldsymbol{\lambda}, t) \equiv \ln\langle e^{\boldsymbol{\lambda}\cdot\mathbf{X}(t)}\rangle$ of the tracer position as [21]

$$\partial_t \Psi(\boldsymbol{\lambda}, t) = \frac{1}{2d\tau} \sum_{\mu} (e^{\sigma \lambda \cdot \hat{\mathbf{e}}_\mu} - 1)[1 - w_{\hat{\mathbf{e}}_\mu}(\boldsymbol{\lambda}, t)]. \quad (1)$$

Here, the sum runs over $\mu \in \{\pm 1, \ldots, \pm d\}$, we called $\hat{\mathbf{e}}_\mu$ the unit vectors along the Cartesian directions, and finally the generalized profile $w_{\mathbf{r}}(\boldsymbol{\lambda}, t) = \langle \rho_{\mathbf{X}+\mathbf{r}} e^{\boldsymbol{\lambda} \cdot \mathbf{X}} \rangle / \langle e^{\boldsymbol{\lambda} \cdot \mathbf{X}} \rangle$ encodes all correlations between the tracer position and the occupations. Equation (1) demonstrates how these correlations completely control the statistical properties of the tracer position. The first among these cross correlations is

$$w_{\mathbf{r}}^{(1)} \equiv \left. \frac{\mathrm{d}w_{\mathbf{r}}}{\mathrm{d}\lambda_1} \right|_{\boldsymbol{\lambda}=\mathbf{0}} = \langle (X_t - \langle X_t \rangle)(\rho_{\mathbf{X}+\mathbf{r}} - \langle \rho_{\mathbf{X}+\mathbf{r}} \rangle) \rangle = \langle X_t \rho_{\mathbf{X}+\mathbf{r}} \rangle, \quad (2)$$

where we indicated without loss of generality $X_t \equiv \mathbf{X} \cdot \hat{\mathbf{e}}_1$ [since $w_{\mathbf{r}}^{(1)}$ can only depend on the relative orientations of $\mathbf{X}$ and $\mathbf{r}$], and where in the last step we used that $\langle X_t \rangle = 0$ and $\langle \rho_{\mathbf{X}+\mathbf{r}} \rangle = \bar{\rho}$. This is the simplest and most physically significant among the TP-bath correlation profiles, and it completely characterizes the variance of the TP [see Eq. (1)]. In the following, we aim at analyzing its spatial properties in the stationary limit attained at long times, and for an infinite system. To this end, we note that an evolution equation for $w_{\mathbf{r}}^{(1)}(t)$ [akin to Eq. (1) for $\Psi(\boldsymbol{\lambda}, t)$] can be obtained starting from the master equation, but it naturally involves higher-order cross-correlation functions [29]. This hierarchy can however be closed by approximating $\langle \rho_{\mathbf{X}+\mathbf{r}} \rho_{\mathbf{X}+\mathbf{r}'} \rangle \simeq \langle \rho_{\mathbf{X}+\mathbf{r}} \rangle \langle \rho_{\mathbf{X}+\mathbf{r}'} \rangle$, and $\langle \delta X_t \rho_{\mathbf{X}+\mathbf{r}} \rho_{\mathbf{X}+\mathbf{r}'} \rangle \simeq \langle \rho_{\mathbf{X}+\mathbf{r}} \rangle \langle \delta X_t \rho_{\mathbf{X}+\mathbf{r}'} \rangle + \langle \delta X_t \rho_{\mathbf{X}+\mathbf{r}} \rangle \langle \rho_{\mathbf{X}+\mathbf{r}'} \rangle$, where $\delta x \equiv x - \langle x \rangle$. Such *decoupling* approximation [20,21,37] goes beyond the simple mean-field [above we only discarded terms of $\mathcal{O}(\delta x^2)$ and $\mathcal{O}(\delta x^3)$, respectively], and has been shown in [22] to become exact both in the dense limit, and in the dilute limit with fixed bath particles. In the same work, this method was used to derive a closed set of self-consistent equations satisfied by $w_{\mathbf{r}}^{(1)}$ for the case of a driven tracer, which were then solved numerically and used to accurately predict the diffusion coefficient of the tracer. Here, we focus instead on the unbiased case, for which we show in [29] that such self-consistent equations can in fact be solved *analytically*. In the stationary limit attained by $w_{\mathbf{r}}^{(1)}(t)$ if $d \geq 2$, the result reads simply

$$w_{\mathbf{r}}^{(1)} = \frac{\sigma \bar{\rho}(1 - \bar{\rho})}{(2 - \bar{\rho})d - (2 - 3\bar{\rho})\mathcal{I}_d(\hat{\mathbf{e}}_1)} \mathcal{I}_d(\mathbf{r}), \quad (3)$$

with $\mathcal{I}_d(\mathbf{r}) = \int_{-\pi}^{\pi} [\mathrm{d}^d q/(2\pi)^d] \{\sin(q_1) \sin(\mathbf{q} \cdot \mathbf{r}) / [1 - (1/d) \sum_{j=1}^{d} \cos(q_j)]\}$. Its asymptotic behavior for large positive $x \equiv \mathbf{r} \cdot \hat{\mathbf{e}}_1$ can then be inspected by standard techniques [29], yielding

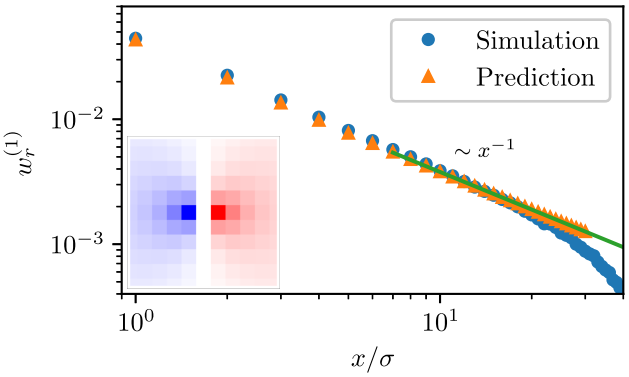

FIG. 2. Stationary tracer-bath correlation profile $w_{\mathbf{r}}^{(1)}$ [see Eqs. (2) and (3)] for the hard-core lattice gas model, as measured from simulations in $d = 2$. Its large-distance tails are characterized by the algebraic behavior (4). In the simulation we used $L = 100$ and $\bar{\rho} = 0.8$. Inset: color map indicating the spatial symmetries of $w_{\mathbf{r}}^{(1)}$ on a square lattice (red means positive while blue means negative).

$$w_{\mathbf{r}}^{(1)} \sim \frac{\sigma \bar{\rho}(1 - \bar{\rho})}{(2 - \bar{\rho})d - (2 - 3\bar{\rho})\mathcal{I}_d(\hat{\mathbf{e}}_1)} \frac{\Gamma(d/2)d}{\pi^{d/2}} x^{1-d}. \quad (4)$$

Note that $w_{-\mathbf{r}}^{(1)} = -w_{\mathbf{r}}^{(1)}$ by symmetry [see Eq. (2)], so that in particular it vanishes for $\mathbf{r} \perp \hat{\mathbf{e}}_1$, see the inset of Fig. 2. Additionally, $w_{\mathbf{r}}^{(1)} > 0$ for $\mathbf{r} \cdot \hat{\mathbf{e}}_1 > 0$, indicating that in a realization where $X_t > 0$ (corresponding to a net displacement to the "right"), the density of particles around the tracer will show an accumulation of particles in the same direction ("in front" of the tracer), and a depletion of particles in the opposite direction ($\mathbf{r} \cdot \hat{\mathbf{e}}_1 < 0$, "behind"). This behavior is tested in Fig. 2 against numerical simulations, showing excellent agreement [while we stress that the prediction (3) is expected to become exact both in the dense and dilute limits]. The simple algebraic decay $w_{\mathbf{r}}^{(1)} \sim x^{1-d}$ is our first main result. Below we consider a system of Brownian particles featuring a substantially distinct type of interaction, and construct an analogous tracer-bath correlation profile, which we then characterize.

Soft interacting Brownian particles—As a second paradigmatic model, we now consider a system of $(N + 1)$ particles at positions $\mathbf{X}_i(t) \in \mathbb{R}^d$ [as in Fig. 1(b)], each evolving according to the overdamped Langevin dynamics

$$\partial_t \mathbf{X}_i(t) = -\mu \sum_{j \neq i} \nabla_{\mathbf{X}_i} U(\mathbf{X}_i(t) - \mathbf{X}_j(t)) + \boldsymbol{\eta}_i(t). \quad (5)$$

Here, the noise terms are Gaussian with zero mean and correlations $\langle \boldsymbol{\eta}_i(t) \boldsymbol{\eta}_j^{\mathrm{T}}(t') \rangle = 2\mu T \delta_{i,j} \delta(t - t') \mathbb{1}$, where we set the Boltzmann constant $k_B = 1$, while $U(\mathbf{x}) = U(|\mathbf{x}|)$ is a pairwise interaction potential. This type of system lends itself to analytical treatment within the Dean-Kawasaki framework [24,25], upon linearization of the effective coarse-grained dynamics. Following [24,26], we first derive

the coupled evolution equations for the tracer position $\mathbf{X}(t) \equiv \mathbf{X}_{i=0}(t)$, and the fluctuating density $\rho(\mathbf{x},t) = \sum_{i=1}^{N} \delta(\mathbf{x} - \mathbf{X}_i(t))$ of the other particles. We then linearize the latter around a fixed background density $\bar{\rho}$ as $\rho(\mathbf{x},t) = \bar{\rho} + \bar{\rho}^{1/2}\phi(\mathbf{x},t)$, according to the prescription $h\phi(\mathbf{x},t) \ll 1$, where $h \equiv 1/\bar{\rho}^{1/2}$. This yields [29]

$$\partial_t \mathbf{X}(t) = -h\mu \nabla_{\mathbf{X}} \mathcal{H}[\phi, \mathbf{X}] + \boldsymbol{\eta}_0(t), \tag{6}$$

$$\partial_t \phi(\mathbf{x},t) = \mu \boldsymbol{\nabla} \cdot \left[\boldsymbol{\nabla} \frac{\delta \mathcal{H}[\phi, \mathbf{X}]}{\delta \phi(\mathbf{x},t)} + \boldsymbol{\xi}(\mathbf{x},t) \right], \tag{7}$$

where $\langle \boldsymbol{\xi}(\mathbf{x},t) \boldsymbol{\xi}^{\mathsf{T}}(\mathbf{x}',t') \rangle = 2\mu T \delta(\mathbf{x} - \mathbf{x}') \delta(t - t') \mathbb{1}$, and with the pseudo-Hamiltonian

$$\mathcal{H}[\phi, \mathbf{X}] = \frac{1}{2} \int \mathrm{d}\mathbf{x}\, \mathrm{d}\mathbf{y}\, \phi(\mathbf{x}) [T\delta(\mathbf{x} - \mathbf{y}) + u(\mathbf{x} - \mathbf{y})] \phi(\mathbf{y}) + h \int \mathrm{d}\mathbf{y}\, \phi(\mathbf{y}) u(\mathbf{y} - \mathbf{X}), \tag{8}$$

where we rescaled $u(\mathbf{x}) = \bar{\rho} U(\mathbf{x})$.

Using Stratonovich calculus, we first derive the relation [29]

$$\partial_t \Psi(\boldsymbol{\lambda}, t) = \lambda^2 \mu T - h\mu \boldsymbol{\lambda} \cdot \int \frac{\mathrm{d}^d q}{(2\pi)^d} \mathrm{i}\mathbf{q} u_{\mathbf{q}} w_{\mathbf{q}}(\boldsymbol{\lambda}, t), \tag{9}$$

where $\Psi(\boldsymbol{\lambda}, t) \equiv \ln \langle \mathrm{e}^{\boldsymbol{\lambda} \cdot \mathbf{X}(t)} \rangle$ as above, and where we denoted $u_{\mathbf{q}} = \int \mathrm{d}^d x\, \mathrm{e}^{-\mathrm{i}\mathbf{q}\cdot\mathbf{x}} u(\mathbf{x})$ the spatial Fourier transform of the interaction potential (which we assume henceforth to exist). The cumulants of the tracer position are thus dictated by the correlations with the particle bath, encoded in the generalized correlation profile $w(\mathbf{x}, \boldsymbol{\lambda}, t) \equiv \langle \phi(\mathbf{x} + \mathbf{X}(t), t) \mathrm{e}^{\boldsymbol{\lambda} \cdot \mathbf{X}(t)} \rangle / \langle \mathrm{e}^{\boldsymbol{\lambda} \cdot \mathbf{X}(t)} \rangle$, in complete analogy with Eq. (1) for the discrete case. We emphasize that these correlation profiles are in general dynamical observables, and as such they are not directly reducible to the usual pair correlation functions predicted and measured for simple liquids [28,38–43]. Again, the first and most relevant among these cross correlations is

$$w^{(1)}(\mathbf{x}, t) \equiv \hat{\mathbf{e}}_1 \cdot \langle \mathbf{X}(t) \phi(\mathbf{x} + \mathbf{X}(t), t) \rangle, \tag{10}$$

i.e., the continuous counterpart of $w_{\mathbf{r}}^{(1)}$ introduced in Eq. (2) for the lattice gas model. In the following, we set out to compute its stationary value $w^{(1)}(\mathbf{x})$ attained in the long-time limit. To this end, we treat perturbatively the term proportional to h in Eq. (8), which controls the interaction between the tracer and the coarse-grained bath density. This corresponds to an expansion around the *soft* interaction limit, as we argue below and in [29]. Working in the Fourier domain, we focus on [44]

$$\partial_t w_{\mathbf{q}}^{(1)}(t) = \left\{ \left\langle \dot{\mathbf{X}}(t)\, \phi_{\mathbf{q}}(t)\, \mathrm{e}^{\mathrm{i}\mathbf{q}\cdot\mathbf{X}(t)} \right\rangle + \left\langle \mathbf{X}(t)\, \dot{\phi}_{\mathbf{q}}(t)\, \mathrm{e}^{\mathrm{i}\mathbf{q}\cdot\mathbf{X}(t)} \right\rangle + \mathrm{i} \left\langle [\mathbf{q} \cdot \dot{\mathbf{X}}(t)]\, \mathbf{X}(t)\, \phi_{\mathbf{q}}(t)\, \mathrm{e}^{\mathrm{i}\mathbf{q}\cdot\mathbf{X}(t)} \right\rangle \right\} \cdot \hat{\mathbf{e}}_1, \tag{11}$$

and we replace $\dot{\mathbf{X}}(t)$ and $\dot{\phi}_{\mathbf{q}}(t)$ on the right-hand side by using the equations of motion (6) and (7). This produces several expectation values, which we compute in [29] within perturbation theory—in particular, the terms involving the Gaussian noises $\boldsymbol{\eta}_0(t)$ and $\boldsymbol{\xi}(\mathbf{x},t)$ can be evaluated within Stratonovich calculus using the Furutsu-Novikov-Donker formula [45–50]. In the stationary limit, we thus find

$$w^{(1)}(\mathbf{x}) = -hT \int \frac{\mathrm{d}^d q}{(2\pi)^d} \frac{\mathrm{e}^{\mathrm{i}\mathbf{q}\cdot\mathbf{x}} \mathrm{i} q_1 u_{\mathbf{q}}}{q^2 (T + u_{\mathbf{q}})(2T + u_{\mathbf{q}})} + \mathcal{O}(h^2). \tag{12}$$

Note that the calculation delineated above can be promptly extended to the case in which the tracer is biased by an external force $\mathbf{f}$, which is obtained by adding a term $\mathbf{f}\delta_{i,0}$ to the right-hand side of Eq. (6). In particular, in [29] we recover by the same method the average density profile $w^{(0)}(\mathbf{x}) = \langle \phi(\mathbf{x} + \mathbf{X}) \rangle$ in the frame of the tracer, which had been previously derived in [26] by distinct techniques.

The large-distance behavior of $w^{(1)}(\mathbf{x})$ in Eq. (12) can be extracted without the need to specify the interaction potential $u_{\mathbf{q}}$. Indeed, in [29] we analyze the singular behavior of $w_{\mathbf{q}}^{(1)}$ around $\mathbf{q} \sim \mathbf{0}$ and show that, for large (positive) $x = \mathbf{x} \cdot \hat{\mathbf{e}}_1$ and in $d \geq 2$,

$$w^{(1)}(x) \sim \frac{hT u_{\mathbf{q}=\mathbf{0}}}{\Omega_d (T + u_{\mathbf{q}=\mathbf{0}})(2T + u_{\mathbf{q}=\mathbf{0}})} x^{1-d}, \tag{13}$$

where Ω_d is the d-dimensional solid angle. Remarkably, $w^{(1)}(x)$ displays the same algebraic decay exponent as the one found in Eq. (4) for the hard-core lattice gas, in spite of the inherently distinct nature of the interparticle interactions in these two models. Besides, also the prefactor in Eq. (13) is largely insensitive to the spatial details of the interaction potential, as it only depends on its typical energy scale via $u_{\mathbf{q}=\mathbf{0}}$ [29]. In Fig. 3(a) we test this prediction for a system of Brownian particles in $d = 2$ interacting via Gaussian pairwise potentials, finding excellent agreement (an analogous test for a smaller system in $d = 3$ is reported in [29]).

Robustness of the algebraic behavior—First, since in our calculation we neglected perturbative terms of $\mathcal{O}(h^2)$ or higher, it is natural to wonder whether the qualitative features of $w^{(1)}(\mathbf{x})$ presented above remain robust away from the limit in which $h = 1/\bar{\rho}^{1/2}$ is small. We verified numerically that this is indeed the case [see, e.g., Fig. 3(a), for which $\bar{\rho} = 0.5$]; even in regimes where discrepancies do show up at short distances, by contrast they hardly affect the large-distance tail (13) of the correlation profile. In fact, in [29] we verify that the validity of perturbation theory is rather linked to the interaction energy being small compared to typical thermal fluctuations, as hinted above and in [26].

Furthermore, the expression (12) relies on the existence of the Fourier transform $u_{\mathbf{q}}$ of the interaction potential. This, together with the use of perturbation theory, in principle

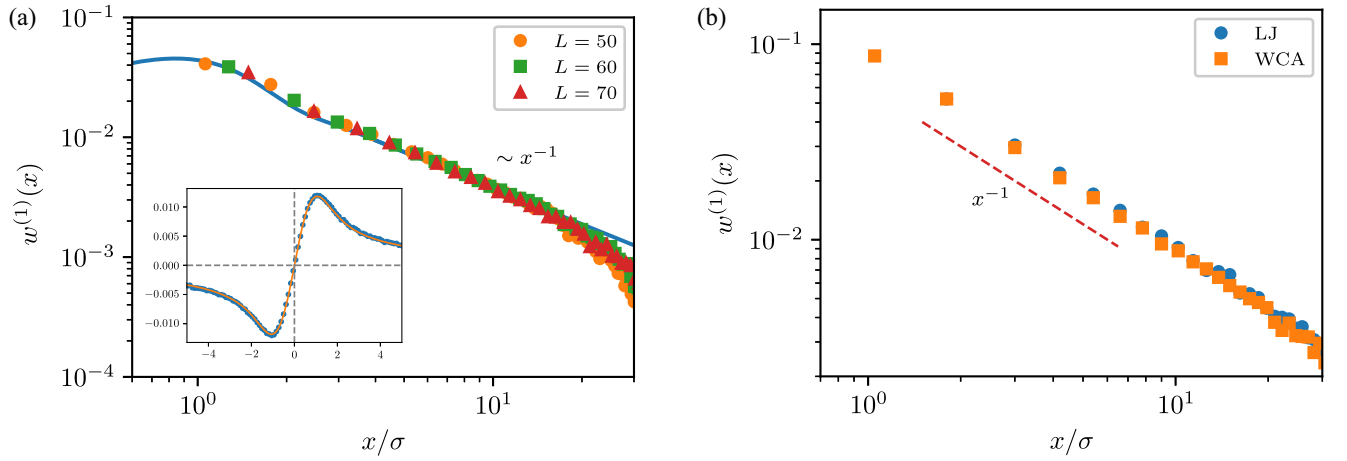

FIG. 3. (a) Stationary correlation profile $w^{(1)}(x)$ for a system of Brownian particles interacting via Gaussian pairwise potentials, i.e., $U(r) = \epsilon \exp[-(r/\sigma)^2]$, in $d = 2$. Its large-distance behavior predicted in Eq. (13) is compared to the result of numerical simulations, obtained with $T = 0.8$, $\bar{\rho} = 0.5$, and for various system sizes (the other parameters were set to unity). The solid line corresponds to the analytic expression (12), computed along $x = \mathbf{r} \cdot \hat{\mathbf{e}}_1$. Inset: check of the accuracy of the prediction at short distances in a system of size $L = 20$ with $\epsilon = 0.1$. In panel (b) we replaced the Gaussian potential by Lennard-Jones and WCA potentials, showing the robustness of the large-distance algebraic decay (the dashed line is a guide to the eye) for potentials not described by the Dean-Kawasaki theory. This simulation was performed in $d = 2$ with $L = 120$; see [29] for additional details.

restricts the applicability of the theory to soft interactions, and excludes strong short-distance repulsion—such as the one typically modeled by Lennard-Jones (LJ) potentials in the description of fluids [28,51]. To test the robustness of the asymptotic algebraic decay predicted for the correlation profile $w^{(1)}(\mathbf{x})$ in Eq. (13), we have thus simulated LJ fluids and measured $w^{(1)}(\mathbf{x})$ numerically. The results in Fig. 3(b) indeed confirm the persistence of this large-distance algebraic behavior. In the simulations we used both LJ and Weeks-Chandler-Andersen (WCA) potentials, the latter corresponding to retaining only the repulsive part of the LJ interaction, and shifting it vertically so that the minimum potential energy is zero [29]. Remarkably, the two curves shown in Fig. 3(b) appear to coincide, provided the typical length and energy scales of the two potentials are chosen to be equal. This is consistent with the prefactor in Eq. (13) depending only on $u_{\mathbf{q}=\mathbf{0}}$, but it is nontrivial in the present context, since the LJ and WCA potentials do not admit a Fourier transform.

Conclusion—In summary, we have characterized the cross-correlation profile between the TP position and the density of surrounding particles, for several paradigmatic interacting particle models. Remarkably, its large-distance algebraic behavior $w^{(1)}(x) \sim x^{1-d}$ turns out to be simple and robust upon changing the details of the pairwise interaction. This decay is faster in higher dimensions, which traces back to the efficiency of the homogenization by the diffusion of the bath particles in high dimensions. Note that, in confined quasi-1d systems such as strips, diffusion is even more efficient, so that the decay is expected to be faster than algebraic (see also [52] for a similar effect on the mean density around a driven tracer).

Our findings pave the way toward the analysis of higher-order correlation profiles, which will be the subject of future work. We expect these and related observables to be accessible using the approach developed in this Letter, where the preliminary calculation of the stationary TP-bath correlation profiles allows one to access the statistical properties of the TP without resorting to the path-integral formalism developed in [53]. For instance, it would be interesting to inspect if the crossover from algebraic to exponential decay of the average density profile $w^{(0)}(\mathbf{x})$, observed in [52] upon spatial confinement of the system, carries over also to the continuum case [54]. Finally, our analysis naturally calls for a unified description of such seemingly different interacting particle systems, which would shed light on the physical origin of the universal behavior that we unveiled in this Letter.

Acknowledgments—D. V. thanks Luca Capizzi and Pietro Luigi Muzzeddu for stimulating discussions.

Data availability—The data that support the findings of this Letter are not publicly available. The data are available from the authors upon reasonable request.

[1] T. M. Squires and T. G. Mason, Fluid mechanics of microrheology, Annu. Rev. Fluid Mech. **42**, 413 (2010).

[2] D. T. Chen, E. R. Weeks, J. C. Crocker, M. F. Islam, R. Verma, J. Gruber, A. J. Levine, T. C. Lubensky, and a. G. Yodh, Rheological microscopy: Local mechanical properties from microrheology, Phys. Rev. Lett. **90**, 108301 (2003).

[3] A. W. C. Lau, B. D. Hoffman, A. Davies, J. C. Crocker, and T. C. Lubensky, Microrheology, stress fluctuations, and active behavior of living cells, Phys. Rev. Lett. **91**, 198101 (2003).

[4] A. M. Puertas and T. Voigtmann, Microrheology of colloidal systems, J. Phys. Condens. Mat. **26**, 243101 (2014).

[5] L. G. Wilson, a. W. Harrison, a. B. Schofield, J. Arlt, and W. C. K. Poon, Passive and active microrheology of hard-sphere colloids, J. Phys. Chem. B **113**, 3806 (2009).

[6] L. G. Wilson, A. W. Harrison, W. C. K. Poon, and A. M. Puertas, Microrheology and the fluctuation theorem in dense colloids, Europhys. Lett. **93**, 58007 (2011).

[7] M. Guo, A. J. Ehrlicher, M. H. Jensen, M. Renz, J. R. Moore, R. D. Goldman, J. Lippincott-Schwartz, F. C. Mackintosh, and D. A. Weitz, Probing the stochastic, motor-driven properties of the cytoplasm using force spectrum microscopy, Cell **158**, 822 (2014).

[8] B. R. Parry, I. V. Surovtsev, M. T. Cabeen, C. S. O'Hern, E. R. Dufresne, and C. Jacobs-Wagner, The bacterial cytoplasm has glass-like properties and is fluidized by metabolic activity, Cell **156**, 183 (2014).

[9] U. M. B. Marconi, A. Puglisi, L. Rondoni, and A. Vulpiani, Fluctuation-dissipation: Response theory in statistical physics, Phys. Rep. **461**, 111 (2008).

[10] P. Langevin, Sur la théorie du mouvement Brownien, Compt. Rendus **146**, 530 (1908).

[11] P. Mazur and I. Oppenheim, Molecular theory of Brownian motion, Physica (Amsterdam) **50**, 241 (1970).

[12] J. L. Lebowitz and E. Rubin, Dynamical study of Brownian motion, Phys. Rev. **131**, 2381 (1963).

[13] T. Chou, K. Mallick, and R. K. P. Zia, Nonequilibrium statistical mechanics: From a paradigmatic model to biological transport, Rep. Prog. Phys. **74**, 116601 (2011).

[14] K. Mallick, The exclusion process: A paradigm for non-equilibrium behaviour, Physica (Amsterdam) **418A**, 17 (2015).

[15] H. Spohn, *Large Scale Dynamics of Interacting Particles* (Springer, Berlin, Heidelberg, 1991).

[16] A. Grabsch, A. Poncet, P. Rizkallah, P. Illien, and O. Bénichou, Exact closure and solution for spatial correlations in single-file diffusion, Sci. Adv. **8**, eabm5043 (2022).

[17] A. Grabsch, P. Rizkallah, A. Poncet, P. Illien, and O. Bénichou, Exact spatial correlations in single-file diffusion, Phys. Rev. E **107**, 044131 (2023).

[18] K. Mallick, H. Moriya, and T. Sasamoto, Exact solution of the macroscopic fluctuation theory for the symmetric exclusion process, Phys. Rev. Lett. **129**, 040601 (2022).

[19] P. Rizkallah, A. Grabsch, P. Illien, and O. Bénichou, Duality relations in single-file diffusion, J. Stat. Mech. (2023) 013202.

[20] O. Bénichou, P. Illien, G. Oshanin, A. Sarracino, and R. Voituriez, Microscopic theory for negative differential mobility in crowded environments, Phys. Rev. Lett. **113**, 268002 (2014).

[21] P. Illien, O. Bénichou, G. Oshanin, and R. Voituriez, Distribution of the position of a driven tracer in a hardcore lattice gas, J. Stat. Mech. (2015) P11016.

[22] P. Illien, O. Bénichou, G. Oshanin, A. Sarracino, and R. Voituriez, Nonequilibrium fluctuations and enhanced diffusion of a driven particle in a dense environment, Phys. Rev. Lett. **120**, 200606 (2018).

[23] O. Bénichou, P. Illien, G. Oshanin, A. Sarracino, and R. Voituriez, Tracer diffusion in crowded narrow channels, J. Phys. Condens. Matter **30**, 443001 (2018).

[24] D. S. Dean, Langevin equation for the density of a system of interacting Langevin processes, J. Phys. A **29**, L613 (1996).

[25] K. Kawasaki, Microscopic analyses of the dynamical density functional equation of dense fluids, J. Stat. Phys. **93**, 527 (1998).

[26] V. Démery, O. Bénichou, and H. Jacquin, Generalized Langevin equations for a driven tracer in dense soft colloids: Construction and applications, New J. Phys. **16**, 053032 (2014).

[27] For instance, this approach is unable to reproduce the subdiffusive behavior expected for hard-core particles in one dimension.

[28] J.-P. Hansen and I. R. McDonald, *Theory of Simple Liquids* (Elsevier, New York, 2013).

[29] See Supplemental Material at http://link.aps.org/supplemental/10.1103/55qy-sflc, which includes Refs. [30–36], for details on the computations and numerical simulations.

[30] B. Hughes, *Random Walks and Random Environments: Random walks*, Oxford Science Publications Vol. 1 (Clarendon Press, 1995), ISBN:9780198537885.

[31] A. Poncet, A. Grabsch, P. Illien, and O. Bénichou, Generalized correlation profiles in single-file systems, Phys. Rev. Lett. **127**, 220601 (2021).

[32] I. S. Gradshteyn and I. M. Ryzhik, *Table of Integrals, Series, and Products*, 7th ed. (Elsevier/Academic Press, Amsterdam, 2007).

[33] U. C. Täuber, *Critical Dynamics: A Field Theory Approach to Equilibrium and Non-equilibrium Scaling Behavior* (Cambridge University Press, Cambridge, England, 2014).

[34] O. Bénichou, A. M. Cazabat, J. De Coninck, M. Moreau, and G. Oshanin, Stokes formula and density perturbances for driven tracer diffusion in an adsorbed monolayer, Phys. Rev. Lett. **84**, 511 (2000).

[35] U. Basu, V. Démery, and A. Gambassi, Dynamics of a colloidal particle coupled to a Gaussian field: From a confinement-dependent to a non-linear memory, SciPost Phys. **13**, 078 (2022).

[36] A. P. Thompson, H. M. Aktulga, R. Berger, D. S. Bolintineanu, W. M. Brown, P. S. Crozier, P. J. in 't Veld, A. Kohlmeyer, S. G. Moore, T. D. Nguyen, R. Shan, M. J. Stevens, J. Tranchida, C. Trott, and S. J. Plimpton, LAMMPS—a flexible simulation tool for particle-based materials modeling at the atomic, meso, and continuum scales, Comput. Phys. Commun. **271**, 108171 (2022).

[37] O. Bénichou, P. Illien, G. Oshanin, and R. Voituriez, Fluctuations and correlations of a driven tracer in a hard-core lattice gas, Phys. Rev. E **87**, 032164 (2013).

[38] R. Evans, J. Henderson, D. Hoyle, A. Parry, and Z. Sabeur, Asymptotic decay of liquid structure: Oscillatory liquid-vapour density profiles and the Fisher-Widom line, Mol. Phys. **80**, 755 (1993).

[39] R. Evans, R. J. F. Leote de Carvalho, J. R. Henderson, and D. C. Hoyle, Asymptotic decay of correlations in liquids and their mixtures, J. Chem. Phys. **100**, 591 (1994).

[40] R. Leote de Carvalho and R. Evans, The decay of correlations in ionic fluids, Mol. Phys. **83**, 619 (1994).
[41] M. Dijkstra and R. Evans, A simulation study of the decay of the pair correlation function in simple fluids, J. Chem. Phys. **112**, 1449 (2000).
[42] P. Hopkins, A. J. Archer, and R. Evans, Asymptotic decay of pair correlations in a Yukawa fluid, Phys. Rev. E **71**, 027401 (2005).
[43] D. Stopper, H. Hansen-Goos, R. Roth, and R. Evans, On the decay of the pair correlation function and the line of vanishing excess isothermal compressibility in simple fluids, J. Chem. Phys. **151**, 014501 (2019).
[44] Since the Gaussian white noises $\boldsymbol{\eta}_0$ and $\boldsymbol{\xi}$ in Eqs. (6) and (7) are additive, we adopt the Stratonovich calculus throughout without loss of generality.
[45] E. A. Novikov, Functionals and the random-force method in turbulence theory, Sov. Phys. JETP **20**, 1290 (1965), http://www.jetp.ras.ru/cgi-bin/dn/e_020_05_1290.pdf.
[46] J. Łuczka, Non-Markovian stochastic processes: Colored noise, Chaos **15**, 026107 (2005).
[47] D. Venturelli, F. Ferraro, and A. Gambassi, Nonequilibrium relaxation of a trapped particle in a near-critical Gaussian field, Phys. Rev. E **105**, 054125 (2022).
[48] D. Venturelli and A. Gambassi, Inducing oscillations of trapped particles in a near-critical Gaussian field, Phys. Rev. E **106**, 044112 (2022).
[49] D. Venturelli and A. Gambassi, Memory-induced oscillations of a driven particle in a dissipative correlated medium, New J. Phys. **25**, 093025 (2023).
[50] D. Venturelli, S. A. M. Loos, B. Walter, É. Roldán, and A. Gambassi, Stochastic thermodynamics of a probe in a fluctuating correlated field, Europhys. Lett. **146**, 27001 (2024).
[51] D. McQuarrie, *Statistical Mechanics* (University Science Books, 2000), ISBN:9781891389153.
[52] O. Bénichou, P. Illien, G. Oshanin, A. Sarracino, and R. Voituriez, Nonlinear response and emerging nonequilibrium microstructures for biased diffusion in confined crowded environments, Phys. Rev. E **93**, 032128 (2016).
[53] V. Démery and D. S. Dean, Perturbative path-integral study of active- and passive-tracer diffusion in fluctuating fields, Phys. Rev. E **84**, 011148 (2011).
[54] D. Venturelli and M. Gross, Tracer particle in a confined correlated medium: An adiabatic elimination method, J. Stat. Mech. (2022) 123210.